chemosensors

MDPI

Article

Synthesis of Quaternary (Ni, Co, Cu)Se_2 Nanosheet Arrays on Carbon Cloth for Non-Enzymatic Glucose Determination

Yuanyuan Chen [1], Huan Wang [2], Huinan Chen [2], Jingyao Song [2], Dongmei Deng [2,*] and Liqiang Luo [1,*]

[1] Department of Chemistry, Shanghai University, Shanghai 200444, China; chenainv33@163.com
[2] Department of Physics, Shanghai University, Shanghai 200444, China; 15093087253@163.com (H.W.); chen_huinan@126.com (H.C.); songjy96@163.com (J.S.)
* Correspondence: dmdeng@shu.edu.cn (D.D.); luck@shu.edu.cn (L.L.); Tel.: +86-21-66132404 (L.L.)

Abstract: Unlike transition metal oxides and sulfides, transition metal-based selenides display higher electrical conductivity, more electroactive unsaturated edge sites, and better chemical stability, which have found extensive usage in electrocatalysis. In this work, simple hydrothermal and solvothermal procedures were employed to synthesize quaternary (Ni, Co, Cu)Se_2 nanosheet arrays on carbon cloth (CC) to measure glucose. The conductivity of the material can be effectively elevated by adding Se element to form selenides, and the synergistic effect between the three selenides can improve the electrocatalytic performance. Consequently, in the ranges of 0.01–600 μM and 600–9000 μM, respectively, the current response of the synthesized material to glucose concentration exhibited linear relationships. The sensor demonstrated excellent sensitivity and a low detection limit of 5.82 nM. Furthermore, the practical applicability of the constructed biosensor was proved by using it to quantify the amount of glucose in human serum.

Keywords: (Ni, Co, Cu)Se_2; carbon cloth; nanosheet arrays; glucose sensor

Citation: Chen, Y.; Wang, H.; Chen, H.; Song, J.; Deng, D.; Luo, L. Synthesis of Quaternary (Ni, Co, Cu)Se_2 Nanosheet Arrays on Carbon Cloth for Non-Enzymatic Glucose Determination. *Chemosensors* **2023**, *11*, 530. https://doi.org/10.3390/chemosensors11100530

Academic Editors: Won-Yong Jeon, Young-bong Choi and Núria Serrano

Received: 26 July 2023
Revised: 18 September 2023
Accepted: 7 October 2023
Published: 9 October 2023

1. Introduction

Glucose is a monosaccharide necessary for metabolism and can directly participate in the metabolic process within the human body [1,2]. It is crucial to the study of biology and serves as the primary source of energy for organisms. The capacity to detect glucose is critical in healthcare and the food sector. Usually, the standard of glucose content in human blood is 3.9–6.1 mM for fasting blood glucose and 5.1–7.0 mM for postprandial blood glucose, while the amount of glucose in human sweat is 10–200 μM. Low glucose levels, however, may result in hypoglycemia or seizures [3]. A chronic metabolic condition characterized by elevated blood glucose is diabetes mellitus. In the meantime, it is also used as a diabetes diagnosis indicator [4,5]. When the levels of glucose in the blood are high for an extended period, it can lead to significant health problems such as nephropathy, retinopathy, and cardiovascular disease [6]. Among these instances, abnormal blood glucose levels in diabetic people may result in issues with apoptosis in addition to certain types of inflammation. To prevent problems with this metabolic disease, blood glucose levels need to be regularly monitored. The requirement for a speedy and precise blood glucose measurement method is of paramount significance given the current rise in the number of diabetic patients worldwide.

Nowadays, with the increasing number of individuals suffering from diabetes, it is critical to come up with swift and effective glucose detection techniques. The electrochemical technique is regarded as the most efficient technique for glucose determination since it is affordable, convenient to operate, and extremely sensitive [7–10]. Currently, both enzyme-based and enzyme-free glucose sensors are applied as electrochemical glucose sensors. Since 1962, due to their excellent specificity, enzyme electrodes have been used to detect blood glucose [11]. In glucose enzymatic sensors, glucose dehydrogenase and oxidase are

frequently utilized. The following features of the glucose–enzyme catalyst are apparent: (a) one enzyme molecule is capable of taking part in one type of reaction as a result of its high specificity; (b) every molecule of the enzyme has a high catalytic efficiency; and (c) enzymes possess extremely specific catalytic requirements. To participate in the procedure, they frequently require to be at normal temperature and pressure [12]. Unfortunately, the vast majority of conventional glucose sensors use natural enzymes as receptors, which severely restricts their practical use due to the drawbacks of natural enzymes, such as easy activity loss, a problematic fixation process, and instability. No matter what enzyme is employed or how the enzyme remains immobilized, enzyme-based electrochemical sensors are unable to offer perfect reproducibility, making their large-scale production and utilization relatively challenging. The detection performance of the enzyme-free glucose electrochemical sensor is marginally worse than that of the conventional glucose enzyme sensor, but it overcomes the dependence on the enzyme, has a wide detection range, good reproducibility, and other advantages. This greatly broadens the public understanding of the sensor. Enzyme-free glucose sensors are more stable, repeatable, and easy to use than enzyme-based glucose sensors [13,14].

As a result of their quick response time, high accuracy, affordable cost, and superior sensitivity, enzyme-free glucose electrochemical sensors have attracted an abundance of attention [15]. One of the most significant variables influencing sensor performance is speculated to be electrode materials. The fabrication of electrode materials with a large surface area, good catalytic capacity, and efficient and precise glucose detection becomes essential. More specifically, by modifying their shape, size, composition, adsorption capacity, electron transport capabilities, and specific surface area, numerous highly efficient materials have been created to enhance sensor performance [16,17]. Numerous metals and metal oxide materials have been employed for glucose-sensing applications throughout the last few decades. Noble metal (Ag, Au, Pd, and Pt) nanomaterials are among them and have been recognized as the best option for creating enzyme-free glucose sensors because of their excellent glucose catalytic effects. The prohibitively costly price of these metals for the creation of enzyme-free glucose sensors, nevertheless, restricts their application [18,19]. Consequently, for the purpose of creating enzyme-free glucose sensors, researchers have employed transition metal composites, particularly the oxides of transition metals, including Ni, Co, Zn, Cu, Mn, Sn, and Zn. Dong et al. employed the hydrothermal approach, for instance, to create reduced graphene oxide (rGO). On the substrate, $NiMn_2O_4$ nanosheets have been produced and utilized to detect glucose electrochemically. The developed $NiMn_2O_4$@rGO sensor might detect glucose with a broad linear range and high sensitivity [20]. It additionally offers good anti-interference and stability. A Co_3O_4 nanowire array and ZnO nanosheet were combined to create a composite electrode by Ye et al. utilizing a straightforward hydrothermal and pulsed electrodeposition technique. With a low detection threshold and a quick response time of only three seconds to glucose amperage, the constructed three-dimensional porous ZnO@Co_3O_4 sensor could selectively detect glucose [7]. In the past few years, transition metals and their compounds have increasingly been applied as suitable electrode materials for sensors [21,22]. Among them, Cu, Co, and Ni are inexpensive. Due to the electron-mediated effect in the redox pairs of Cu^{2+}/Cu^{3+}, Co^{2+}/Co^{3+}, and Ni^{2+}/Ni^{3+}, Cu-Co-Ni-based micro-nanomaterials can serve as efficient electrocatalysts for glucose oxidation in alkaline media [20,23]. In addition, the unique synergistic effects among multiple metals can provide multiple opportunities to improve their electrocatalytic performance. The majority of multi-metal catalysts, per the literature, perform catalytically far superior to mono-metal catalysts [24]. Consequently, Cu, Co, and Ni trimetal-based electrode materials are highly desirable for applications in glucose electroanalysis.

Currently, nanomaterials such as transition metal oxides [25], sulfides [26], and hydroxides [27] are widely used in glucose electrochemical sensors. In the periodic table of elements, oxygen, sulfur, and selenium have similar properties. Compared with oxygen and sulfur, selenium has an increased ionic radius and a decreased electronegativity [28].

Consequently, selenides exhibit enhanced polarizability, more electroactive unsaturated edge sites, and improved electrical conductivity and redox activity [29,30]. The advantages, as mentioned earlier, are additionally valid for the enzyme-based electrochemical sensing of glucose. Harish et al. used a one-step hydrothermal method to synthesize Cu_2Se. The constructed Cu_2Se sensor possesses excellent sensitivity and a low detection limit, permitting it to detect glucose in physiological bodily fluids in smaller amounts [31]. Ma et al. described the in situ fabrication of nickel selenide (Ni_3Se_2) nanosheet arrays on nickel foam (NF) and how they were utilized as an enzyme-free glucose sensor. With a detection range from 0.25 μM to 6.33 mM, the Ni_3Se_2/NF electrode demonstrated a high efficiency for electrocatalytic glucose oxidation [32]. Xu et al. synthesized rock-like $NiSe_2$ nanoparticles on carbon nanorods using a simple thermal treatment method [33]. The unique core–shell structure of $NiSe_2$/carbon nanorods increased the catalytic area and active sites, and the introduction of Se improved the charge transfer rate. The resulting glucose biosensor, comprising $NiSe_2$ and carbon nanorods, displayed a broad linear range, excellent sensitivity, and a modest detection limit. Wang et al. prepared CoSe on carbon nanosheets with NaCl-assisted pyrolysis [34]. The sensor exhibited good selectivity and a wide linear range in detecting glucose.

In this work, we used straightforward hydrothermal and solvothermal techniques to successfully synthesize homogeneous (Ni, Co, Cu)Se_2 nanosheet arrays on carbon cloth (CC). The nanosheet morphology of (Ni, Co, Cu)Se_2 could offer more active areas and increase the kinetics of the reaction. Moreover, the synergistic effect of the three metals Cu, Co, and Ni improved the electrocatalytic performance of (Ni, Co, Cu)Se_2. Thus, the fabricated (Ni, Co, Cu)Se_2/CC electrode exhibited outstanding capability for the electrochemical oxidation of glucose. In addition, human serum samples were used to evaluate the potential application of the constructed sensor.

2. Materials and Methods

2.1. Chemicals

We purchased CC (hydrophilic, WOS1009) from Cetech Co., Ltd. in Taiwan, China. $Co(NO_3)_2{\cdot}6H_2O$, $Cu(NO_3)_2{\cdot}3H_2O$, NaCl, $Ni(NO_3)_2{\cdot}6H_2O$, NaOH, $NaBH_4$, and selenium were bought from Sinopharm Chemical Reagent Co., Ltd. in Shanghai, China. Shanghai Macklin Biochemical Co., Ltd. in Shanghai, China, provided fructose (Fru), ammonium fluoride (NH_4F), urea (CH_4N_2O), sucrose (Suc), and D-(+)-glucose (Glu). Sigma-Aldrich (St Louis, MO, USA) supplied dopamine (DA), uric acid (UA), maltose (Mal), ascorbic acid (AA), and glycine (Gly). Shanghai University Hospital provided serum. The entire experiment was conducted using deionized water (18.25 M cm).

2.2. Apparatus

Through the use of scanning electron microscopy (SEM, SU5000, Japan) and energy dispersive X-ray spectroscopy (EDS), the surface morphology and chemical elemental content of the samples were examined. With high-resolution transmission electron microscopy (HRTEM, JEM-2100F, JEOL, Japan), more details on the tiny crystal structure were revealed. Using X-ray diffraction (XRD, DLMAX-2200, Cu target, K rays, Japan), the crystal structure of samples was identified. X-ray photoelectron spectroscopy (XPS, ESCALAB 250 XI, USA) examined the chemical makeup of the samples and the valence state. The electrochemical performance of synthetic materials was tested on an electrochemical workstation (CHI 660 D, Shanghai, China) utilizing (Ni, Co, Cu)Se_2/CC as the working electrode and Ag/AgCl (saturated KCl) and platinum wire as the reference and counter electrodes, respectively.

2.3. Synthesis of (Ni, Co, Cu)-LDH on CC

The precursor layered double hydroxide ((Ni, Co, Cu)-LDH) was fabricated on CC as follows: To prepare CC (2 cm × 3 cm) for usage, it was first ultrasonically cleaned for 15 min in a solution of ethanol, 0.5 M HCl, and deionized water. In 40 mL of water, stirring was used to dissolve 0.291 g $Co(NO_3)_2{\cdot}6H_2O$, 0.581 g $Ni(NO_3)_2{\cdot}6H_2O$, and 0.241 g

$Cu(NO_3)_2 \cdot 3H_2O$. The solution was then used to dissolve 0.148 g NH_4F and 0.480 g urea. Afterwards, a 50 mL autoclave was used to hydrothermally react the resulting solution and the pretreated CC for 6 h at 150 °C. After the reaction was finished, it was removed and washed in turns using ethanol and water. (Ni, Co, Cu)-LDH/CC was obtained after drying in a vacuum oven at 60 °C. Additionally, LDH arrays with ratios of 1:1:1, 1:1:3, 1:1:4, and 1:1:5 were prepared by adjusting the molar ratio of Cu:Co:Ni.

2.4. Synthesis of (Ni, Co, Cu)Se_2 on CC

The selenization of fabricated precursors was processed using the solvothermal method to obtain (Ni, Co, Cu)Se_2/CC. In 3 mL of water, 0.059 g selenium powder and 0.065 g $NaBH_4$ were dissolved. Fresh NaHSe solution was made after 10 min of stirring, and 60 mL of absolute ethanol was added after 10 min of N_2 flow to stop NaHSe oxidation. After that, the mixture and the precursor were put into a 100 mL autoclave and then heated to 140 °C for 12 h. Later, the samples were exposed to Ar gas while being calcined for 2 h at 350 °C.

3. Results and Discussion

3.1. Structure and Morphology Characterization of (Ni, Co, Cu)Se_2/CC

Figure 1 depicts a schematic diagram of the (Ni, Co, Cu)Se_2/CC synthesis process. First, the hydrothermal technique was used to create precursor (Ni, Co, Cu)-LDH nanosheets on CC with a Cu: Co: Ni ratio of 1:1:2 (Figure 2a). Then, the precursors were selenized using the solvothermal method. By comparing Figure 2a,b, the morphology of (Ni, Co, Cu)Se_2 nanosheets can be clearly seen after the selenization of the precursor using the solvothermal method. Figure S1 shows the SEM images of LDHs fabricated from other Cu: Co: Ni salts with different ratios. The (Ni, Co, Cu)-LDH precursor was then reacted using fresh NaHSe as the Se source to create the appropriate metal selenides. As indicated in Figure S2, the precursors prepared from Cu: Co: Ni salt ratios of 1:1:1, 1:1:3, 1:1:4, and 1:1:5 exhibited large-area agglomeration after selenization. However, the (Ni, Co, Cu)Se_2 obtained after selenization from the precursor with a Cu: Co: Ni ratio of 1:1:2 was still nanosheet-like, with some particles attached to the surface. This could result from specific precursors remaining partially separated during the selenization procedure and subsequently aggregating to produce particles on the surface of the nanosheets. Furthermore, the elements of (Ni, Co, Cu)Se_2 were explored using EDS with SEM. The proportion of Co, Ni, Cu, and Se elements is 16%, 29%, 29%, and 25%, respectively. From Figure 2d, it is apparent that Ni, Co, Cu, and Se elements were dispersed with equal regard. The microstructure of the (Ni, Co, Cu)Se_2 nanosheets was investigated with TEM. The TEM image (Figure 2e) reconfirms the nanosheet structure of (Ni, Co, Cu)Se_2. Following the (311) crystal plane of the (Ni, Co, Cu)Se_2 substance, the high-resolution TEM (Figure 2f) reveals that the lattice fringe spacing was 0.181 nm.

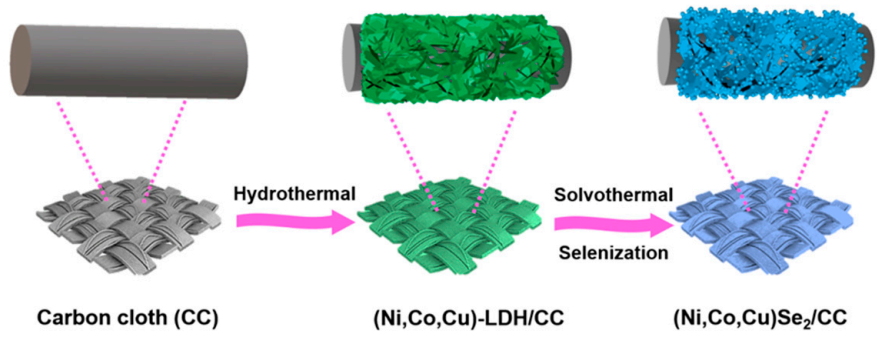

Figure 1. Schematic illustration of the synthetic procedure of (Ni, Co, Cu)Se_2/CC.

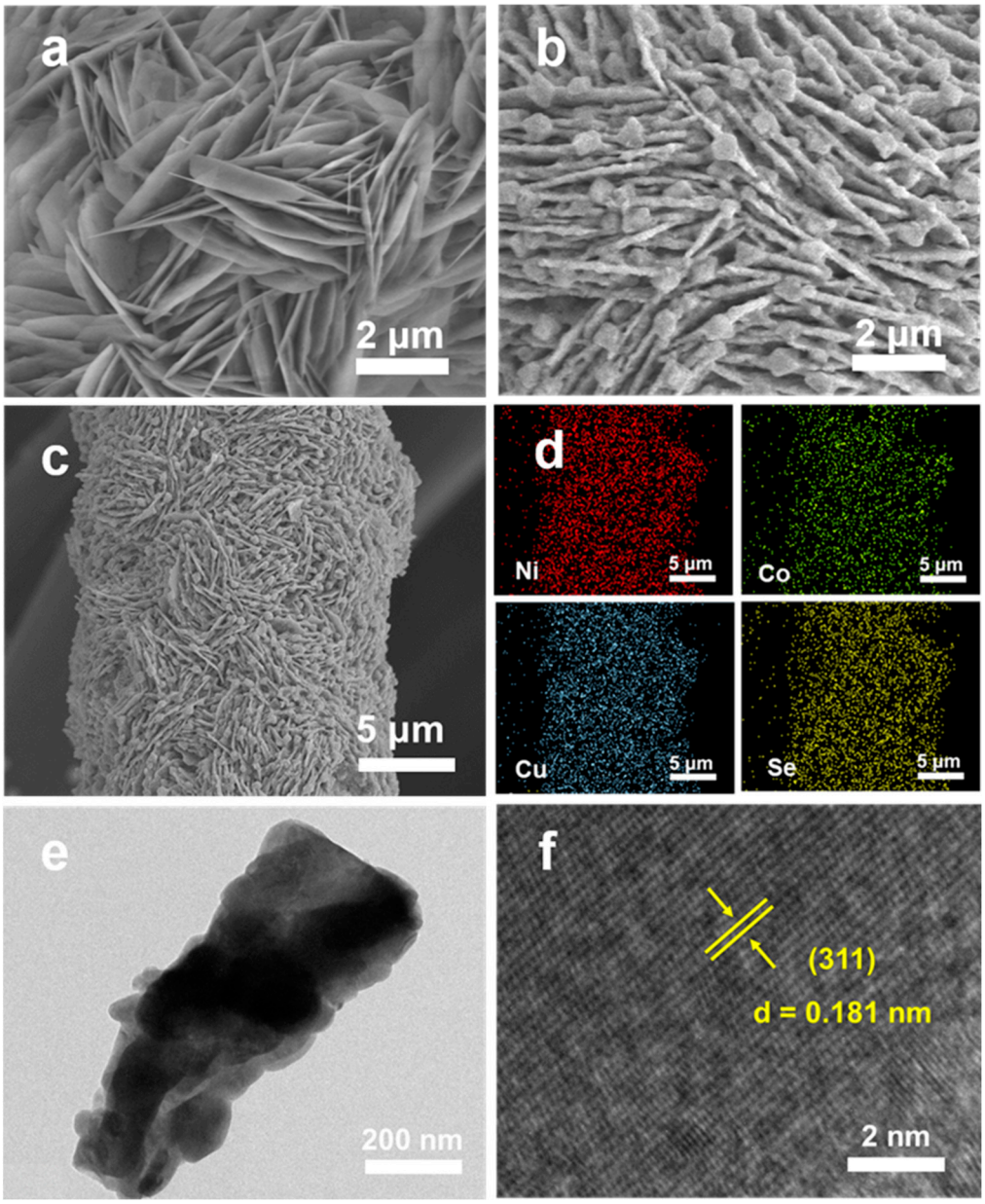

Figure 2. (**a**) SEM image of (Ni, Co, Cu)-LDH. (**b**,**c**) SEM and (**d**) elemental mapping images of (Ni, Co, Cu)Se_2 microspheres. (**e**) TEM and (**f**) high-resolution TEM images of (Ni, Co, Cu)Se_2.

The crystal structure of (Ni, Co, Cu)Se_2/CC was determined with XRD. The obtained diffraction peaks were consistent with the cubic (Ni, Co, Cu)$(Se, S)_2$ phase (JCPDS No. 29–1417). As depicted in Figure 3a, the (200), (210), (211), (220), (311), (230), (321), (400), (421), and (332) planes of (Ni, Co, Cu)$(Se, S)_2$ can be identified by the diffraction peaks, which have the following coordinates: 30.3°, 34.0°, 37.4°, 43.4°, 51.4°, 56.3°, 58.6°, 63.1°, and 75.6° [15]. Therefore, it can be proved that the synthesized sample is Ni/Co/Cu selenide. In addition, the diffraction peak observed at 26.3° corresponds to CC. XPS was used to study the constitutions and element chemical valence states of the (Ni, Co, Cu)Se_2/CC. The survey scan spectrum shown in Figure 3b contained the characteristic peaks for the Ni, Cu, Co, Se, and C elements. Figure 3c presents the XPS spectra of Cu 2p with a satellite peak at 943.27 eV. The peaks at 933.12 and 952.98 eV, which correspond to the Cu^0/Cu^+ state, exhibit the distribution of Cu $2p_{3/2}$ and Cu $2p_{1/2}$. Cu^{2+} species are believed to be responsible for the peaks at 935.16 and 954.87 eV [35,36]. The Ni 2p XPS spectra are displayed in Figure 3d. The satellite peaks at 861.56 and 881.15 eV are attributed to Ni $2p_{3/2}$

and Ni $2p_{1/2}$ of Ni^{2+}, respectively [37,38]. Co $2p_{3/2}$ and Co $2p_{1/2}$ of Co^{2+} are identified by the peaks at 781.55 and 796.15 eV in the XPS spectra of Co 2p (Figure 3e), and the associated satellite peaks are located at 786.97 and 803.69 eV [39,40]. The Se 3d spectra in Figure 3f exhibit peaks at 54.82 and 55.93 eV that are associated with Se $3d_{5/2}$ and Se $3d_{3/2}$, respectively. In contrast, the sizable sharp peak at 59.02 eV is correlated with SeO_x and may be carried forth by the surface oxidation of selenides [41–43].

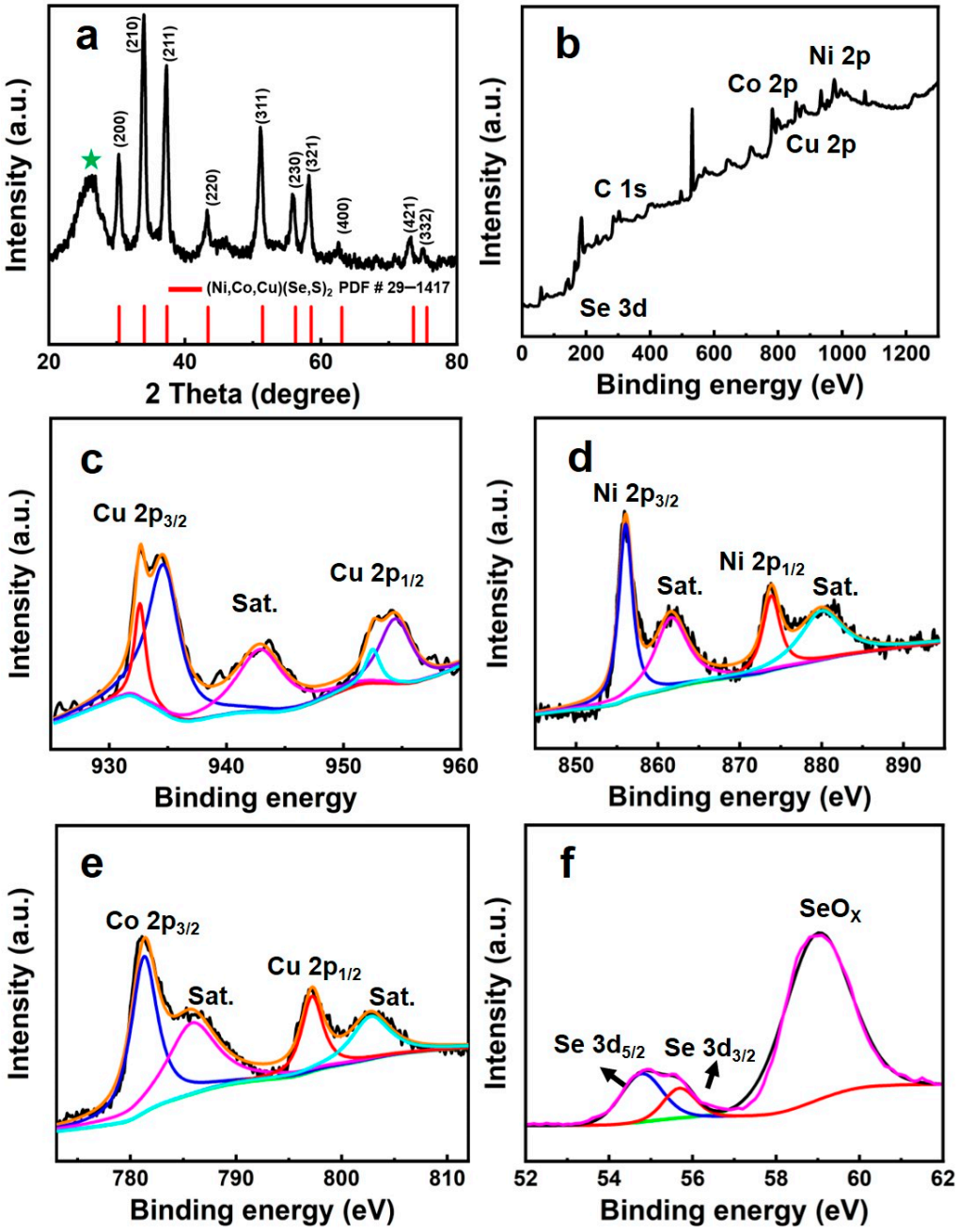

Figure 3. (**a**) XRD diffraction patterns of (Ni, Co, Cu)Se_2/CC. (**b**–**f**) XPS spectra of Cu 2p, Ni 2p, Co 2p, and Se 3d for (Ni, Co, Cu)Se_2/CC, respectively.

3.2. Electrochemical Performance of (Ni, Co, Cu)Se_2/CC

Using cyclic voltammetry (CV) in an alkaline solution, the electrocatalytic property of (Ni, Co, Cu)Se_2/CC was examined. As depicted in Figure 4a, the CV curves of bare CC, (Ni, Co, Cu)-LDH/CC, and (Ni, Co, Cu)Se_2/CC electrodes were tested at a scan rate of 50 mV s^{-1} either with or without the addition of 2 mM glucose to 0.1 M NaOH solution.

Due to the inferior catalytic efficiency, even in glucose, there was no response for the bare CC. The superior electrocatalytic activity of (Ni, Co, Cu)Se_2/CC was discovered based on the excellent current response compared to (Ni, Co, Cu)-LDH/CC. As depicted in Figure S3, the electrochemical behaviors of CoSe, NiSe, CuSe, and (Ni, Co, Cu)Se_2 in response to glucose in 0.1 M NaOH were examined. When 2 mM glucose was introduced, the oxidation current density produced by (Ni, Co, Cu)Se_2 was significantly higher than that produced by CoSe, NiSe, and CuSe due to the synergistic effect between the various metals accelerating the electron transport speed and enhancing the electrochemical performance of the sensor.

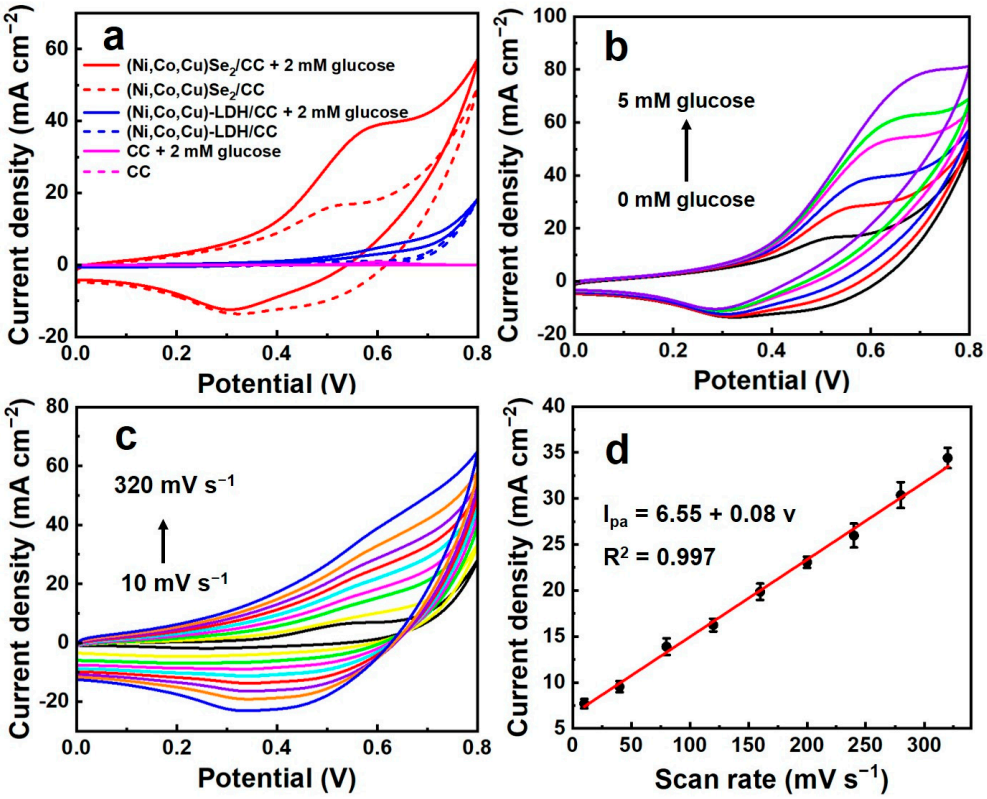

Figure 4. (**a**) The CVs of CC, (Ni, Co, Cu)-LDH/CC, and (Ni, Co, Cu)Se_2/CC in the presence and absence of 2 mM glucose (solid line and dashed line, respectively). (**b**) CVs of (Ni, Co, Cu)Se_2/CC at 0–5 mM glucose in 0.1 M NaOH at a scan rate of 50 mV s^{-1}. (**c**) CVs of (Ni, Co, Cu)Se_2/CC in 0.1 M NaOH containing 1 mM glucose at various scan rates (10–320 mV s^{-1}). (**d**) The scan rate response and peak current response linear relationship calibration curve.

To improve the sensing capacity of (Ni, Co, Cu)Se_2/CC, the concentration of NaOH and the applied voltage were optimized using the current–time method. Figure 5a shows the response current curves of (Ni, Co, Cu)Se_2/CC catalyzing 0.1 mM glucose with different concentrations of NaOH as the supporting electrolyte. The response current peaked in the 0.1 M NaOH concentration and then rapidly declined when the NaOH concentration increased further. As a result, 0.1 M NaOH was determined to be the optimal electrolyte solution. The response current curves of (Ni, Co, Cu)Se_2/CC catalyzing 0.1 mM glucose at various applied voltages are shown in Figure 5b. With the increase in applied voltage in the range from 0.45 to 0.60 V, the response current also increased. Therefore, the subsequent experiments were conducted with a 0.1 M NaOH solution and 0.6 V applied voltage.

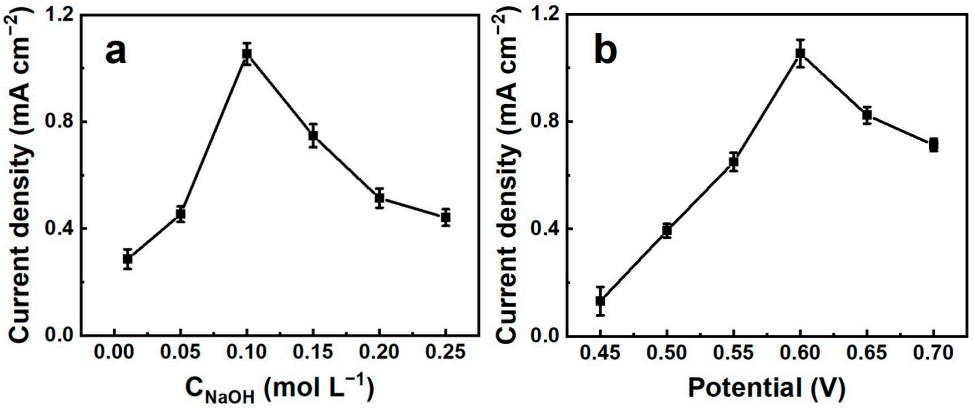

Figure 5. 0.1 mM glucose current response: effects of experimental parameters. (**a**) NaOH concentration. (**b**) Applied potential.

The CVs of (Ni, Co, Cu)Se_2/CC were measured in a 0.1 M NaOH solution that had varying glucose concentrations. As can be seen in Figure 4b, as glucose concentration rose, the oxidation current also rose. In addition, the oxidation current was proportional to the glucose concentration, implying that (Ni, Co, Cu)Se_2/CC with superior electrocatalytic activity was suitable as the electrode material for the electrochemical sensing of glucose. The impact of scan rate and kinetic analysis were additionally examined in a solution of 0.1 M NaOH with 1.0 mM glucose at scanning rates ranging from 10 to 320 mV s^{-1}. (Figure 4c). Figure 4d shows that the oxidation peak current rose as the scanning rate rose, and the relationship appeared linear, demonstrating an electrode reaction controlled by adsorption [28,44]. In an alkaline solution, Cu (II) was combined with OH^- to form the strong oxidizing agent CuOOH (III). Then, glucose was oxidized to glucoselactone by CuOOH (III) [23,45,46]. The mechanism of electrocatalytic oxidation of glucose in (Ni, Co, Cu)Se_2/CC may be explained by the following chemical equations:

$$\text{Ni (II)} + 3OH^- \leftrightarrow \text{NiOOH (III)} + H_2O + e^-$$

$$\text{Co (II)} + 3OH^- \leftrightarrow \text{CoOOH (III)} + H_2O + e^-$$

$$\text{Cu (II)} + 3OH^- \leftrightarrow \text{CuOOH (III)} + H_2O + e^-$$

$$\text{NiOOH (III)} + \text{glucose} \rightarrow Ni(OH)_2\ \text{(II)} + \text{gluconolactone}$$

$$\text{CoOOH (III)} + \text{glucose} \rightarrow Co(OH)_2\ \text{(II)} + \text{gluconolactone}$$

$$\text{CuOOH (III)} + \text{glucose} \rightarrow Cu(OH)_2\ \text{(II)} + \text{gluconolactone}$$

The electrochemical active surface area (ECSA) of the electrode was evaluated from the CVs. The ECSA is proportional to the double layer capacitance (C_{dl}), and the ECSA calculation is more complicated, so the ECSA of the electrode is compared by calculating the C_{dl}. The electrochemical double layer capacitance is calculated according to the formula $i_c = \nu C_{dl}$, where ν is the sweep speed, i_c is one half of the difference between the oxidation current and the reduction current, and $i_c = (i_{pa} - i_{pc})/2$. In order to calculate the i_c relatively accurately, an intermediate value is selected to calculate the difference between the oxidation current and the reduction current. The CVs of the material at potentials of 0–0.1 V were examined utilizing multiple scan rates (20–160 mV s^{-1}) to determine the electrochemical C_{dl}, being employed to gain access to the electrochemically active specific surface area of the material. The C_{dl} of CC is 1.06 mF cm^{-2}, whereas that of (Ni, Co,

Cu)Se_2/CC is 10.05 mF cm^{-2}, as depicted in Figure 6, demonstrating that the (Ni, Co, Cu)Se_2/CC electrode encounters a rougher surface and is more exposed to active sites. Therefore, the (Ni, Co, Cu)Se_2/CC electrode displays outstanding electrocatalytic capacity. The following two factors may be responsible for the outstanding electrocatalytic activity of (Ni, Co, Cu)Se_2/CC: (1) the high inherent electrical conductivity and abundant redox reactions caused by the valence electron contact exists among the d orbitals of the Ni, Cu, and Co atoms; (2) the catalytic performance was substantially enhanced with the design of quaternary (Ni, Co, Cu)Se_2 nanosheet arrays.

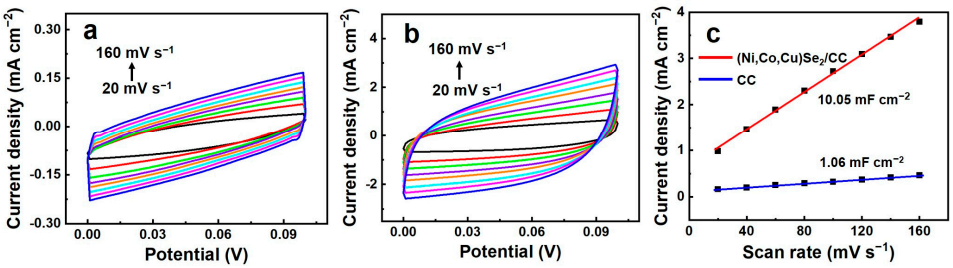

Figure 6. (**a**,**b**) CVs of CC and (Ni, Co, Cu)Se_2/CC electrodes measured in the applied potential range from 0.0 to 0.1 V at various scan rates from 20 to 160 mV s^{-1}. (**c**) The capacitive current at 0.05 V as the function of scan rate for CC and (Ni, Co, Cu)Se_2/CC.

The current–time approach was used to assess the sensitivity and detectable range of the electrochemical catalysis of glucose by (Ni, Co, Cu)Se_2/CC. Figure 7a displays the current–time curves of (Ni, Co, Cu)Se_2/CC while 0.1 M NaOH solution continues to be injected with varying glucose concentrations. In the ranges of 0.01–600 µM and 600–9000 µM, the response currents were linearly connected with glucose concentration. The equations for linearity can be fitted as follows: I (mA cm^{-2}) = 0.21 + 11.45C (mM) (R^2 = 0.992) and I (mA cm^{-2}) = 5.88 + 6.27 C (mM) (R^2 = 0.990), respectively. The corresponding sensitivities are 11.45 mA mM^{-1} cm^{-2} and 6.72 mA mM^{-1} cm^{-2}. Additionally, based on calculations, the glucose detection limit was 5.82 nM. The (Ni, Co, Cu)Se_2/CC electrode showed greater sensitivity at low glucose concentrations and decreased sensitivity at high glucose concentrations. This might be because the glucose oxidation active sites on the electrode surface are partially covered by reaction intermediates that have adhered to the electrode surface, decreasing the sensitivity of the electrode [47]. Moreover, the performance comparison of the proposed (Ni, Co, Cu)Se_2/CC and other reported electrochemical sensors is listed in Table 1. The proposed (Ni, Co, Cu)Se_2/CC electrode presents remarkable performances in the linear range, sensitivity, and detection limit among several samples.

Table 1. Comparison of the (Ni, Co, Cu)Se_2/CC with some previously reported sensors for the detection of glucose.

Modified Material	Linear Range (µM)	Detection Limit (µM)	Sensitivity (µA mM^{-1} cm^{-2})	Reference
CeO_2@CuO	1–89	0.019	3319.83	[45]
$CuCo_2O_4$/CC	1–930	0.5	3930	[48]
CuS/Cu_2O/CuO/Cu	20–4096	0.89	4262	[49]
Ni@Cu-MOF	5–2500	1.67	1703.33	[23]
Co_3O_4-$NiCo_2O_4$	1–2100	0.112	1463.13	[50]
Ni/Cu	0.5–2500	0.05	3924	[51]
$NiSe_2$/cellulose paper	100–1000	24.8	250	[52]
Cu_2-xSe	up to 3375	50	536	[53]
$CuCo_2O_4$	0.01–800	0.003	654.23	[54]
CoSe–rGO [a]	up to 10,000	2.5	480	[55]
(Ni, Co, Cu)Se_2/CC	0.01–600 600–9000	0.00582	11,450 6720	This work

[a] Reduced graphene oxide.

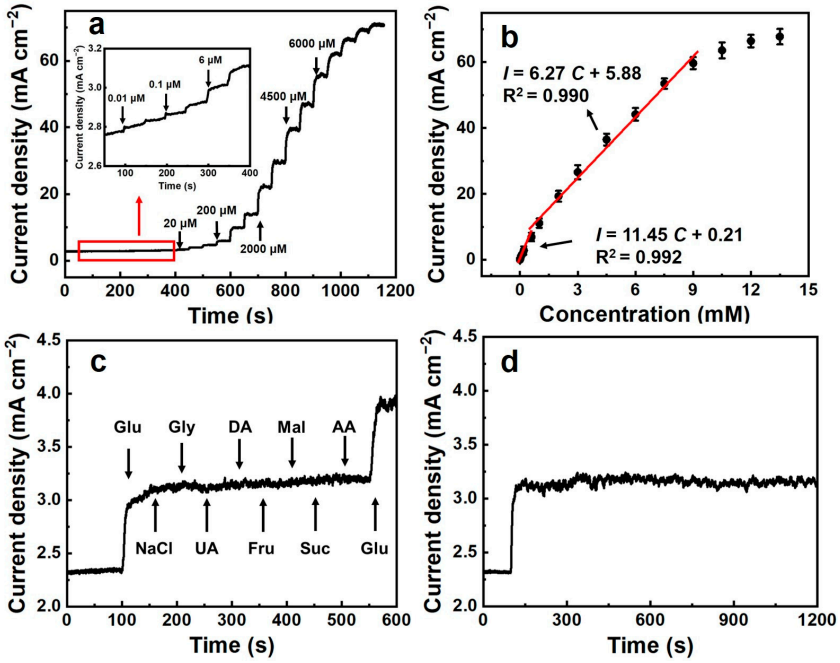

Figure 7. (**a**) Typical amperometric response (I-t) of (Ni, Co, Cu)Se_2/CC with continuous addition of various glucose concentrations. (**b**) The associated calibration curve. (**c**) Selectivity of (Ni, Co, Cu)Se_2/CC toward glucose. (**d**) Current variation in (Ni, Co, Cu)Se_2/CC in 0.1 mM glucose during the 1200 s test time in 0.1 M NaOH at 0.60 V.

3.3. Selectivity, Stability, Repeatability, and Reproducibility Investigation of (Ni, Co, Cu)Se_2/CC

Due to the complexity of biological systems, the selectivity of the electrode constitutes a crucial consideration for the utilization of glucose electrochemical sensors for practical purposes. By testing 0.01 mM of multiple interference-causing chemicals, the selectivity and anti-interference capacity of the (Ni, Co, Cu)Se_2/CC electrode was investigated. As depicted in Figure 7c, the response current of the (Ni, Co, Cu)Se_2/CC electrode to interferents was negligible compared to glucose. Hence, the exceptional selectivity of the (Ni, Co, Cu)Se_2/CC electrode could be proven. Furthermore, the stability of the prepared electrodes was evaluated. As depicted in Figure 7d, the response current of the (Ni, Co, Cu)Se_2/CC electrode to 0.1 mM glucose decreased slightly within 1200 s, indicating that the proposed sensor has excellent stability. Repeatability and reproducibility were also essential factors to evaluate the potential applicability of the sensor. The CVs of the same (Ni, Co, Cu)Se_2/CC electrode were tested against 1 mM glucose six times under identical conditions. As displayed in Figure S4a, the peak current had a relative standard deviation (RSD) as low as 2.1%, indicating excellent repeatability of the electrode. To check the reproducibility of (Ni, Co, Cu)Se_2/CC, six electrodes were tested in 0.1 M NaOH containing 1 mM glucose. As presented in Figure S4b, the peak current has an RSD as low as 1.9%, indicating satisfactory reproducibility of the electrode.

3.4. Real Sample Analysis

Serum analysis is a practical way to identify some disease indices. The level of glucose in human serum was measured utilizing the standard addition method to ascertain the practical usability of the constructed sensor. All serum samples were obtained from the hospital at Shanghai University. Three different human blood samples were centrifuged at 4000 rpm/min at 4 °C for 10 min to separate the supernatant to obtain serum. The current response to adding 20 μM glucose was detected. Each serum sample was retaken three times to confirm the accuracy of the experiment. The outcomes are displayed in Table 2. The recoveries were 101.2, 99.4, and 102.1%, respectively, demonstrating that the suggested sensor may be utilized for detecting glucose in actual serum samples.

Table 2. Determination of glucose in human serum.

Serum Sample	Detected (μM)	Added (μM)	Found (μM)	Recovery (%)	RSD (%)
1	9.40	20	29.64	101.2	0.68
2	14.21	20	34.09	99.4	1.83
3	16.01	20	36.43	102.1	0.97

4. Conclusions

Uniform (Ni, Co, Cu)Se_2 nanosheet arrays were successfully synthesized on CC utilizing hydrothermal and solvothermal processes. The synergistic effect among the three metals Cu, Co, and Ni can effectively improve the catalytic ability of the (Ni, Co, Cu)Se_2/CC electrode for glucose oxidation. In addition, selenides have higher electrical conductivity compared to other chalcogenides. The proposed (Ni, Co, Cu)Se_2/CC sensor exhibits a wide linear range, significantly inferior detection limit, and superior stability. Additionally, the studied sensor has outstanding anti-interference capabilities and has been utilized to determine the amount of glucose in serum samples, implying that the proposed sensor is promising in clinical glucose tests.

Supplementary Materials: The following supporting information can be downloaded at https://www.mdpi.com/article/10.3390/chemosensors11100530/s1, Figure S1: (a–d) SEM images of (Ni, Co, Cu)-LDH arrays with Cu:Co:Ni ratios of 1:1:1, 1:1:3, 1:1:4, and 1:1:5; Figure S2: (a–d) SEM images of (Ni, Co, Cu)Se_2 arrays with Cu:Co:Ni ratios of 1:1:1, 1:1:3, 1:1:4, and 1:1:5; Figure S3: Response curves of (Cu, Co, Ni)Se_2/CC, CoSe/CC, CuSe/CC, and NiSe/CC to the addition of 0 mM and 2 mM glucose in 0.1 M NaOH solution; Figure S4: The repeatability (a) and reproductivity (b) of (Ni, Co, Cu)Se_2/CC electrode to glucose sensing.

Author Contributions: Conceptualization, Y.C.; methodology, Y.C.; discussed the results and corrected the paper draft, Y.C.; writing—review and editing, H.W.; investigation, H.C.; formal analysis, J.S.; supervision, D.D. and L.L.; project administration, L.L.; funding acquisition, D.D. and L.L. All authors have read and agreed to the published version of the manuscript.

Funding: This research was funded by the National Natural Science Foundation of China (grant numbers 62171268 and 61971274).

Institutional Review Board Statement: Not applicable.

Informed Consent Statement: Not applicable.

Data Availability Statement: Not applicable.

Conflicts of Interest: The authors declare no conflict of interest.

References

1. Rani, S.D.; Ramachandran, R.; Sheet, S.; Aziz, M.A.; Lee, Y.S.; Al-Sehemi, A.G.; Pannipara, M.; Xia, Y.; Tsai, S.Y.; Ng, F.L.; et al. $NiMoO_4$ nanoparticles decorated carbon nanofiber membranes for the flexible and high performance glucose sensors. *Sens. Actuators Chem.* **2020**, *312*, 127886. [CrossRef]
2. Fu, R.; Lu, Y.; Ding, Y.; Li, L.; Ren, Z.; Si, X.; Wu, Q. A novel non-enzymatic glucose electrochemical sensor based on CNF@Ni-Co layered double hydroxide modified glassy carbon electrode. *Microchem. J.* **2019**, *150*, 104106. [CrossRef]
3. Shen, M.; Li, W.; Chen, L.; Chen, Y.; Ren, S.; Han, D. NiCo-LDH nanoflake arrays-supported Au nanoparticles on copper foam as a highly sensitive electrochemical non-enzymatic glucose sensor. *Anal. Chim. Acta* **2021**, *1177*, 338787. [CrossRef] [PubMed]
4. Murugan, P.; Annamalai, J.; Atchudan, R.; Govindasamy, M.; Nallaswamy, D.; Ganapathy, D.; Reshetilov, A.; Sundramoorthy, A.K. Electrochemical sensing of glucose using glucose oxidase/PEDOT:4-sulfocalix [4]arene/MXene composite modified electrode. *Micromachines* **2022**, *13*, 304. [CrossRef] [PubMed]
5. Sha, R.; Vishnu, N.; Badhulika, S. MoS_2 based ultra-low-cost, flexible, non-enzymatic and non-invasive electrochemical sensor for highly selective detection of uric acid in human urine samples. *Sens. Actuators Chem.* **2019**, *279*, 53–60. [CrossRef]
6. Wei, M.; Qiao, Y.X.; Zhao, H.T.; Liang, J.; Li, T.S.; Luo, Y.L.; Lu, S.Y.; Shi, X.F.; Lu, W.B.; Sun, X.P. Electrochemical non-enzymatic glucose sensors: Recent progress and perspectives. *Chem. Commun.* **2020**, *56*, 14553–14569. [CrossRef]
7. Ye, Z.; Miao, R.; Miao, F.; Tao, B.; Zang, Y.; Chu, P.K. 3D nanoporous core-shell ZnO@Co_3O_4 electrode materials for high-performance supercapacitors and nonenzymatic glucose sensors. *J. Electroanal. Chem.* **2021**, *903*, 115766. [CrossRef]

8. Shin, J.H.; Lee, M.J.; Choi, J.H.; Song, J.A.; Kim, T.H.; Oh, B.K. Electrochemical H_2O_2 biosensor based on horseradish peroxidase encapsulated protein nanoparticles with reduced graphene oxide-modified gold electrode. *Nano Converg.* **2020**, *7*, 39. [CrossRef]
9. He, Q.G.; Wang, B.; Liang, J.; Liu, J.; Liang, B.; Li, G.L.; Long, Y.H.; Zhang, G.Y.; Liu, H.M. Research on the construction of portable electrochemical sensors for environmental compounds quality monitoring. *Mater. Today Adv.* **2023**, *17*, 100340. [CrossRef]
10. Ayres, L.D.; Brooks, U.J.; Whitehead, K.; Garcia, C.D. Rapid detection of staphylococcus aureus using paper-derived electrochemical biosensors. *Anal. Chem.* **2022**, *94*, 16847–16854. [CrossRef]
11. Clark, L.C.; Lyons, C. Electrode systems for continuous monitoring in cardiovascular surgery. *Ann. N. Y. Acad. Sci.* **1962**, *102*, 29–45. [CrossRef] [PubMed]
12. Naikoo, G.A.; Salim, H.; Hassan, I.U.; Awan, T.; Arshad, F.; Pedram, M.Z.; Ahmed, W.; Qurashi, A. Recent advances in non-enzymatic glucose sensors based on metal and metal oxide nanostructures for diabetes management: A review. *Front. Chem.* **2021**, *11*, 452. [CrossRef] [PubMed]
13. Puttananjegowda, K.; Takshi, A.; Thomas, S. Silicon carbide nanoparticles electrospun nanofibrous enzymatic glucose sensor. *Biosens. Bioelectron.* **2021**, *186*, 113285. [CrossRef] [PubMed]
14. Li, G.; Chen, D.; Chen, Y.; Dong, L. MOF Ni-BTC derived Ni/C/graphene composite for highly sensitive non-enzymatic electrochemical glucose detection. *ECS J. Solid State Sci. Technol.* **2021**, *9*, 121014. [CrossRef]
15. Liu, T.; Zhang, X.; Fu, K.; Su, Z. Fabrication of $Co_3O_4/NiCo_2O_4$ nanocomposite for detection of H_2O_2 and dopamine. *Biosensors* **2021**, *11*, 452. [CrossRef]
16. Wang, D.; Cai, D.; Huang, H.; Liu, B.; Wang, L.; Liu, Y.; Li, H.; Wang, Y.; Li, Q.; Wang, T. Non-enzymatic electrochemical glucose sensor based on $NiMoO_4$ nanorods. *Nanotechnology* **2015**, *26*, 145501. [CrossRef]
17. Chen, T.W.; Ramachandran, R.; Chen, S.M.; Anushya, G.; Ramachandran, K. Graphene and perovskite-based nanocomposite for both electrochemical and gas sensor applications: An overview. *Sensors* **2020**, *20*, 6755. [CrossRef]
18. Wang, Y.; Chen, J.; Zhou, C.; Zhou, L.; Kong, Y.; Long, H.; Zhong, S. A novel self-cleaning, non-enzymatic glucose sensor working under a very low applied potential based on a Pt nanoparticle-decorated TiO_2 nanotube array electrode. *Electrochim. Acta* **2014**, *115*, 269–276. [CrossRef]
19. Xu, X.; Lv, H.; Sun, L.; Song, P.; Liu, B.; Chen, X. An Electrochemical non-enzymatic glucose sensor based on ultrathin PdAg single-crystalline nanowires. *ChemPlusChem* **2020**, *85*, 970–976. [CrossRef]
20. Dong, M.; Hu, H.; Ding, S.; Wang, C.; Li, L. Fabrication of $NiMn_2O_4$ nanosheets on reduced graphene oxide for non-enzymatic detection of glucose. *Mater. Technol.* **2020**, *36*, 203–211. [CrossRef]
21. Lin, L.; Weng, S.; Zheng, Y.; Liu, X.; Ying, S.; Chen, F.; You, D. Bimetallic PtAu alloy nanomaterials for nonenzymatic selective glucose sensing at low potential. *J. Electroanal. Chem.* **2020**, *865*, 114147. [CrossRef]
22. Wang, W.; Dong, Y.; Xu, L.; Dong, W.; Niu, X.; Lei, Z. Combining bimetallic-alloy with selenium functionalized carbon to enhance electrocatalytic activity towards glucose oxidation. *Electrochim. Acta* **2017**, *244*, 16–25. [CrossRef]
23. Xue, Z.; Jia, L.; Zhu, R.R.; Du, L.; Zhao, Q.H. High-performance non-enzymatic glucose electrochemical sensor constructed by transition nickel modified Ni@Cu-MOF. *J. Electroanal. Chem.* **2020**, *858*, 113783. [CrossRef]
24. Li, X.; Wu, H.; Guan, C.; Elshahawy, A.M.; Dong, Y.; Pennycook, S.J.; Wang, J. $(Ni,Co)Se_2$/NiCo-LDH core/shell structural electrode with the cactus-like $(Ni,Co)Se_2$ core for asymmetric supercapacitors. *Small* **2019**, *15*, 1803895. [CrossRef]
25. Wang, H.; Li, Y.; Deng, D.; Li, M.; Zhang, C.; Luo, L. NiO-coated $CuCo_2O_4$ nanoneedle arrays on carbon cloth for non-enzymatic glucose sensing. *ACS Appl. Nano Mater.* **2021**, *4*, 9821–9830. [CrossRef]
26. Wang, H.; Wang, C.; Qing, C.; Sun, D.; Wang, B.; Qu, G.; Sun, M.; Tang, Y. Construction of carbon-nickel cobalt sulphide hetero-structured arrays on nickel foam for high performance asymmetric supercapacitors. *Electrochim. Acta* **2015**, *174*, 1104–1112. [CrossRef]
27. Liu, W.; Xie, J.; Guo, Y.; Lou, S.; Gao, L.; Tang, B. Sulfurization-induced edge amorphization in copper-nickel-cobalt layered double hydroxide nanosheets promoting hydrazine electro-oxidation. *J. Mater. Chem. A* **2019**, *7*, 24437–24444. [CrossRef]
28. Sakthivel, M.; Sukanya, R.; Chen, S.M.; Pandi, K.; Ho, K.C. Synthesis and characterization of bimetallic nickel-cobalt chalcogenides ($NiCoSe_2$, $NiCo_2S_4$, and $NiCo_2O_4$) for non-enzymatic hydrogen peroxide sensor and energy storage: Electrochemical properties dependence on the metal-to-chalcogen composition. *Renew. Energy* **2019**, *138*, 139–151. [CrossRef]
29. Younas, W.; Naveed, M.; Cao, C.; Khalid, S.; Rafai, S.; Wang, Z.; Wu, Y.; Yang, L. Rapid and simplistic microwave assisted method to synthesise cobalt selenide nanosheets: A prospective material for high performance hybrid supercapacitor. *Appl. Surf. Sci.* **2020**, *505*, 144618. [CrossRef]
30. Song, W.; Teng, X.; Liu, Y.; Wang, J.; Niu, Y.; He, X.; Zhang, C.; Chen, Z. Rational construction of self-supported triangle-like MOF-derived hollow $(Ni, Co)Se_2$ arrays for electrocatalysis and supercapacitors. *Nanoscale* **2019**, *11*, 6401–6409. [CrossRef]
31. Singh, H.; Bernabe, J.; Chern, J.; Nath, M. Copper selenide as multifunctional non-enzymatic glucose and dopamine sensor. *J. Mater. Res.* **2021**, *36*, 1413–1424. [CrossRef]
32. Ma, M.; Zhu, W.; Zhao, D.; Ma, Y.; Hu, N.; Suo, Y.; Wang, J. Surface engineering of nickel selenide nanosheets array on nickel foam: An integrated anode for glucose sensing. *Sens. Actuators B Chem.* **2019**, *278*, 110–116. [CrossRef]
33. Xu, Z.; Wang, Q.; Li, R.; Zhangsun, H.; Dong, M.; Wang, L. Surface selenylation engineering for construction of a hierarchical $NiSe_2$/carbon nanorod: A high-performance nonenzymatic glucose sensor. *ACS Appl. Mater. Interfaces* **2021**, *13*, 22866–22873. [CrossRef] [PubMed]

34. Wang, D.; Chang, Y. The construct $CoSe_2$ on carbon nanosheets as high sensitivity catalysts for electro-catalytic oxidation of glucose. *Nanomaterials* **2022**, *12*, 572. [CrossRef] [PubMed]
35. Cao, X.; Johnson, E.; Nath, M. Identifying high-efficiency oxygen evolution electrocatalysts from Co-Ni-Cu based selenides through combinatorial electrodeposition. *J. Mater. Chem. A* **2019**, *7*, 9877–9889. [CrossRef]
36. Chen, B.; Tian, Y.; Yang, Z.; Jiang, J.; Wang, C. Construction of (Ni, Cu)Se_2/reduced graphene oxide for high energy density asymmetric supercapacitor. *ChemElectroChem* **2017**, *4*, 3004–3010. [CrossRef]
37. Du, Y.; Zhao, H.; Wang, W.; Yang, Y.; Wang, M.; Li, S.; Liu, Y.; Wang, L. (Ni,Co)Se@$Ni(OH)_2$ heterojunction nanosheets as an efficient electrocatalyst for the hydrogen evolution reaction. *Dalton Trans.* **2021**, *50*, 391–397. [CrossRef]
38. Sun, C.; Guo, X.; Zhang, J.; Han, G.; Gao, D.; Gao, X. Rechargeable Zn-air batteries initiated by nickel-cobalt bimetallic selenide. *J. Energy Chem.* **2019**, *38*, 34–40. [CrossRef]
39. Liu, Y.L.; Yan, C.; Wang, G.G.; Li, F.; Kang, Q.; Zhang, H.Y.; Han, J.C. Selenium-rich nickel cobalt bimetallic selenides with core-shell architecture enable superior hybrid energy storage devices. *Nanoscale* **2020**, *12*, 4040–4050. [CrossRef]
40. Zhang, Z.; Liu, Y.; Ren, L.; Zhang, H.; Huang, Z.; Qi, X.; Wei, X.; Zhong, J. Three-dimensional-networked Ni-Co-Se nanosheet/nanowire arrays on carbon cloth: A flexible electrode for efficient hydrogen evolution. *Electrochim. Acta* **2016**, *200*, 142–151. [CrossRef]
41. Fan, C.Y.; Zhang, X.H.; Shi, Y.H.; Xu, H.Y.; Zhang, J.P.; Wu, X.L. Three-dimensional hierarchical Ni_3Se_2 nanorod array as binder/carbon-free electrode for high-areal-capacity Na storage. *Nanoscale* **2018**, *10*, 18942–18948. [CrossRef] [PubMed]
42. Li, J.; Yan, D.; Lu, T.; Yao, Y.; Pan, L. An advanced CoSe embedded within porous carbon polyhedra hybrid for high performance lithium-ion and sodium-ion batteries. *Chem. Eng. J.* **2017**, *325*, 14–24. [CrossRef]
43. Song, W.; Wang, K.; Jin, G.; Wang, Z.; Li, C.; Yang, X.; Chen, C. Two-Step hydrothermal synthesis of CoSe/$MoSe_2$ as hydrogen evolution electrocatalysts in acid and alkaline electrolytes. *ChemElectroChem* **2019**, *6*, 4842–4847. [CrossRef]
44. Zhong, Y.; Shi, T.; Liu, Z.; Cheng, S.; Huang, Y.; Tao, X.; Liao, G.; Tang, Z. Ultrasensitive non-enzymatic glucose sensors based on different copper oxide nanostructures by in-situ growth. *Sens. Actuators Chem.* **2016**, *236*, 326–333. [CrossRef]
45. Dayakar, T.; Rao, K.V.; Bikshalu, K.; Malapati, V.; Sadasivuni, K.K. Non-enzymatic sensing of glucose using screen-printed electrode modified with novel synthesized CeO_2@CuO core shell nanostructure. *Biosens. Bioelectron.* **2018**, *111*, 166–173.
46. Ye, J.; Deng, D.; Wang, Y.; Luo, L.; Qian, K.; Cao, S.; Feng, X. Well-aligned Cu@C nanocubes for highly efficient nonenzymatic glucose detection in human serum. *Sens. Actuators B Chem.* **2020**, *305*, 127473. [CrossRef]
47. Guo, S.; Zhang, C.; Yang, M.; Wang, L.; Li, R.; Ma, N. Three-dimensional flexible polyurethane decorated with Ni and reduced graphene oxide for high-sensitive sensing of glucose. *Mater. Chem. Phys.* **2022**, *278*, 125679. [CrossRef]
48. Luo, X.; Huang, M.; Bie, L.; He, D.; Zhang, Y.; Jiang, P. $CuCo_2O_4$ nanowire arrays non-enzymatic glucose sensing. *RSC Adv.* **2017**, *7*, 23093–23101. [CrossRef]
49. Wei, C.; Zou, X.; Liu, Q.; Li, S.; Kang, C.; Xiang, W. A highly sensitive non-enzymatic glucose sensor based on CuS nanosheets modified Cu_2O/CuO nanowire arrays. *Electrochim. Acta* **2020**, *334*, 135630. [CrossRef]
50. Chen, D.; Pang, D.; Zhang, S.; Song, H.; Zhu, W.; Zhu, J. Synergistic coupling of $NiCo_2O_4$ nanorods onto porous Co_3O_4 nanosheet surface for tri-functional glucose, hydrogen-peroxide sensors and supercapacitor. *Electrochim. Acta* **2020**, *330*, 135326. [CrossRef]
51. Liu, S.; Zhao, J.; Qin, L.; Liu, G.; Zhang, Q.; Li, J. Fabrication of Ni/Cu ordered bowl-like array film for the highly sensitive nonenzymatic detection of glucose. *J. Mater. Sci.* **2019**, *55*, 337–346. [CrossRef]
52. Vishnu, N.; Sahatiya, P.; Kong, C.Y.; Badhulika, S. Large area, one step synthesis of $NiSe_2$ films on cellulose paper for glucose monitoring in bio-mimicking samples for clinical diagnostics. *Nanotechnology* **2019**, *30*, 355502. [CrossRef] [PubMed]
53. Hao, X.; Jia, J.; Chang, Y.; Jia, M.; Wen, Z. Monodisperse copper selenide nanoparticles for ultrasensitive and selective non-enzymatic glucose biosensor. *Electrochim. Acta* **2019**, *327*, 135020. [CrossRef]
54. Cui, S.; Gu, S.; Ding, Y.; Zhang, J.; Zhang, Z.; Hu, Z. Hollow mesoporous $CuCo_2O_4$ microspheres derived from metal organic framework: A novel functional materials for simultaneous H_2O_2 biosensing and glucose biofuel cell. *Talanta* **2018**, *178*, 788–795. [CrossRef] [PubMed]
55. Cooray, M.C.D.; Zhang, X.; Zhang, Y.; Langford, S.J.; Bond, A.; Zhang, J. Cobalt selenide nanoflake decorated reduced graphene oxide nanocomposite for efficient glucose electro-oxidation in alkaline medium. *J. Mater. Chem. A* **2017**, *5*, 19289–19296. [CrossRef]